Conserved accessory genes link a phylogenetically distinct *Bacillus subtilis* strain from Indian bekang to the Japanese natto clade

Kiyohiko Seki[1] & Yukio Nagano[1,2,3,4*]

[1]*Faculty of Agriculture, Saga University, Saga, Japan.*

[2]*The United Graduate School of Agricultural Sciences, Kagoshima University, Kagoshima, Japan*

[3]*Vishnu Institute of Pharmaceutical Education & Research, Telangana, India*

[4]*Shri Vishnu College of Pharmacy, Andhra Pradesh, India*

***Corresponding authors:**

E-mail: nagano@cc.saga-u.ac.jp

Abstract

Bacillus subtilis is central to Asian fermented soybean foods, including Japanese natto. To explore the genomic boundaries of *B. subtilis* var. *natto*, we conducted a comparative pangenome analysis of 42 strains, including the core natto clade (n=26) and its closest relatives. Our analysis revealed a striking evolutionary paradox centered on a single strain isolated from Indian bekang. Core-genome phylogenetic analysis places this bekang strain clearly outside the tight natto clade, with a Nepalese kinema strainbeing its closest systematic neighbor. In stark contrast, quantitative analysis of accessory gene profiles revealed this single bekang strain is the functional nearest neighbor to the natto clade, sharing a highly conserved accessory gene repertoire. This shared profile defines a "natto-type" adaptive strategy (the "broad-sense natto group," n=27), separating it from other related strains. Analysis of this group-specific repertoire revealed an enrichment of transcriptional regulators and metabolic enzymes. This finding provides a compelling case study (n=1) of polygenic adaptation, suggesting complex evolutionary pathways, such as horizontal gene transfer or selective retention, can drive rapid adaptation across disparate lineages.

Keywords: *Bacillus subtilis*, Pangenome analysis, Fermented soybean foods, Polygenic adaptation, Niche adaptation

Introduction

Soybeans are a globally important protein source and have been a primary ingredient in a diverse array of Asian fermented foods for centuries, including staples like soy sauce, miso, tempeh, fǔrǔ, and douchi[1]. Fermentation not only boosts the nutritional value and shelf life of soybeans but also imparts unique flavors and functionalities, profoundly enriching regional food cultures. Central to the production of many of these soybean products is *Bacillus subtilis*[2]. This bacterium plays a pivotal role in creating foods like Japanese natto, bekang from India and Myanmar, Korean cheonggukjang, and Nepalese kinema[2]. In these foods, *B. subtilis* is crucial for breaking down soy proteins and carbohydrates, thereby generating umami compounds, distinct aromas, and, in some cases, viscous substances such as polyglutamic acid (PGA)[2,3].

The properties of these foods, and the *B. subtilis* strains that produce them, vary significantly. Strains used for Japanese natto (produced by *B. subtilis* var. *natto*) and Korean cheonggukjang are extensively researched[4,5]. Phenotypically, natto is characterized by its intense, PGA-derived viscosity, whereas cheonggukjang is generally much less viscous. In contrast, other regional foods like Indian bekang are far less documented[6,7]. Bekang is a traditional food consumed in Mizoram, India, and adjacent areas. Critically, despite the scarcity of research, a report indicates that bekang, much like natto, is also characterized by significant viscosity and stringiness, a trait linked to PGA production[7].

This striking convergence of a key phenotype (viscosity) in geographically distant foods (Japanese natto and Indian bekang) makes a genomic comparison particularly compelling. Our research, therefore, focuses on the industrially and culturally significant *B. subtilis* var. *natto* clade. A fundamental question remains: What defines the genomic boundary of this important industrial clade? That is, what genomic features (particularly in the accessory genome) distinguish the natto clade from its phylogenetically closest relatives? Understanding this boundary is key to unraveling the evolutionary mechanisms that led to this specific niche adaptation. Recent advances in genomics

now provide access to sequence information for many *B. subtilis* strains, enabling this focused comparison[6,8,9,10,11,12,13,14,15,16,17,18,19,20,21,22,23,24,25,26,27,28].

To unravel these genetic relationships, pangenome analysis offers a powerful framework[29,30,31]. This method dissects the collective genome of a microbial population into 'core genes' (reflecting vertical evolution and phylogeny) and 'accessory genes' (reflecting niche adaptation). While broad pangenome studies of the *B. subtilis* species group exist[32,33], their large scale is not optimized for resolving the fine-grained genomic differences between a specific industrial clade (like *B. subtilis* var. *natto*) and its immediate sister groups.

This distinction raises a fundamental question, now applied with greater focus: Do the phylogenetic relationships inferred from core genes necessarily align with the accessory gene profiles that reflect adaptation to the nutritional niche of soybean fermentation? This refers to the specific selective pressures of an environment characterized by high concentrations of soy proteins and carbohydrates, requiring efficient enzymatic degradation.

Therefore, the objective of this study was to specifically target the *B. subtilis* var. *natto* clade and its closest relatives to address this question. Our goal was to compare the systematic boundary of the natto clade (defined by core-genome phylogeny) with its functional boundary (defined by accessory-gene profiles). We sought to determine if the phylogenetically nearest neighbor to the natto clade was also its functionally nearest neighbor, or if a discrepancy existed, which would suggest complex evolutionary pathways such as polygenic adaptation.

In pursuing this objective, we made a remarkable discovery centered on a single *B. subtilis* strain isolated from Indian bekang. We report here this compelling case study, which presents a genomic paradox: this single strain, while clearly phylogenetically distinct from the *B. subtilis* var. *natto* clade, exhibits a striking functional similarity based on a shared accessory gene repertoire. As we will

demonstrate, this finding provides a key insight into the complex evolutionary pathways of microbial niche adaptation.

Results

Initial Genome Collection and Overall Pangenome Structure

To explore the genomic diversity surrounding the *B. subtilis* var. *natto* lineage, we initially assembled a dataset of 55 *B. subtilis* genomes, selected based on DNA sequence similarity searches using *B. subtilis* var. *natto* sequences as queries and relevant literature. This initial collection is detailed in Table 1. The set includes numerous strains from Asian fermented food production, alongside several environmental isolates, intended for an exploratory analysis to identify a focal group for deeper investigation. All genomes met high-quality standards for completeness and contamination (Supplementary Table 1). Exploratory pangenome analysis of the 55 strains revealed a large and open pangenome (Supplementary Figure 1). The pangenome size consistently increased with the addition of new genomes, indicating significant genetic diversity. Conversely, the core genome stabilized at approximately 3,000 genes.

Focusing the Analysis on the Natto Clade and Its Relatives

Our primary interest lies in the industrially important natto strains. Exploratory phylogenetic (core-genome tree) and functional (accessory-gene cluster, based on Jaccard distance) analyses of all 55 strains (Supplementary Figures 2, 3, and 4) were conducted. However, neither analysis showed clear, distinct boundaries separating all strains into discrete groups. As the primary objective of this study is to compare the *B. subtilis* var. *natto* clade with its closest relatives, we focused our main analysis on a subset of these strains. We first identified a highly homogeneous, tight-knit clade (n=26) containing all *B. subtilis* var. *natto* strains, which we hereafter refer to as the "narrow-sense natto group". To create a relevant comparison set, we selected an additional 16 strains (for a total of 42) that were relatively close to the natto clade in both exploratory analyses and were also isolated from fermented soybean foods. The remaining 13 strains were excluded from the main analysis as

they were either phylogenetically or functionally distant from the natto clade, and this set also included a relatively high number of environmental isolates.

Core-Genome Phylogeny Reveals a Systematic "Nearest Neighbor"

We constructed a core-genome phylogenetic tree for the 42 strains (Figure 1, Supplementary Figure 5). This tree clearly separates the "narrow-sense natto group" (n=26) from the other 16 related strains. Notably, within this related set, the strain isolated from Nepalese kinema (Food_NPL_1) is positioned as the systematic nearest neighbor (the most recent outgroup) to the "narrow-sense natto group" clade. The Indian bekang isolate (Food_IND_1) is placed more distantly within this related group, clearly separated from the "narrow-sense natto group".

Accessory Genome Clustering Reveals a Contradictory "Functional Nearest Neighbor"

Intriguingly, even a visual inspection of the gene presence/absence matrix associated with the 42-strain core-genome tree (Figure 1, Supplementary Figure 5) provides an intuitive hint that the bekang strain (Food_IND_1), despite its phylogenetic position, shares a profile somewhat similar to the narrow-sense natto group. To formally and quantitatively assess these functional relationships, we performed hierarchical clustering on the 42 strains based on their accessory gene presence/absence profiles using Jaccard distance as the metric (Figure 2). This quantitative analysis revealed a striking paradox. The resulting cluster map (Figure 2) shows a large, functionally similar cluster corresponding to the "narrow-sense natto group" (n=25). However, the functional nearest neighbor (the most recent outgroup) to this cluster is not the systematic nearest neighbor (Food_NPL_1). Instead, it is the Indian bekang isolate (Food_IND_1). The bekang strain, which is phylogenetically more distant (Figure 1, Supplementary Figure 5), is functionally more similar to the "narrow-sense natto group" than any other strain in this set. The systematic nearest neighbor

(Food_NPL_1), despite its close phylogenetic relationship (Figure 1), clusters immediately outside the functional group formed by the "narrow-sense natto group" and the bekang strain in the accessory gene analysis (Figure 2).This clear "discrepancy" — where the systematic nearest neighbor (Food_NPL_1) and the functional nearest neighbor (Food_IND_1) are not the same strain — forms the central finding of this study. This quantitative analysis was used as an exploratory map to assess functional similarity, rather than to define statistically discrete groups.

Synteny and Phylogenetic Network Analyses

To investigate the genomic basis for the functional similarity despite phylogenetic distance, we performed a chromosome-wide synteny analysis comparing representative strains with available chromosome-level genome sequences (Figure 3, Supplementary Figure 6). We selected the natto strain Food_JPN_7 ("narrow-sense natto group"), the bekang strain Food_IND_1, and the doenjang strain Food_KOR_9 ("natto-related group"). The results revealed relatively fewer insertions and deletions (indels) between Food_JPN_7 and Food_IND_1, compared to the significantly larger number of indels between the Food_JPN_7/Food_IND_1 pair and Food_KOR_9. A similar pattern of fewer indels between the natto/bekang pair compared to the bekang/related-group pair was observed when using another available chromosome-level genome from the "natto-related group," Food_KOR_11 (Supplementary Figure 6).

Next, we investigated whether recombination could explain the similarity. We constructed a phylogenetic network from the core genome alignment for the 42 strains (Figure 4, Supplementary Figure 7). We did not detect a clear reticulate signal connecting the bekang isolate (Food_IND_1) directly to the "narrow-sense natto group". However, the analyses did reveal complex relationships among other strains, suggesting recombination and HGT have occurred within this population. Of

particular interest was evidence of recombination between the bekang isolate and the *B. subtilis* strain (Food_MMR_1) from Myanmar, regions which share a geographical border.

Identification and Functional Analysis of Group-Specific Accessory Genes

Based on the results above, we defined two additional operational groups for the subsequent functional comparison. The 15 strains phylogenetically related to the natto group but excluding the bekang strain are referred to as the "natto-related group". The functionally defined cluster, consisting of the "narrow-sense natto group" (n=26) plus the single bekang isolate (Food_IND_1), is termed the "broad-sense natto group" (n=27 total).

To characterize the functional differences, we extracted genes specific to the "broad-sense natto group" (n=27) and the "natto-related group" (n=15). We defined "nearly group-specific genes" using a criterion of ≥80% presence within the target group and ≤20% presence in the comparison group. Using this criterion, we identified 184 nearly specific genes for the broad-sense natto group (Dataset 1) and 83 for the natto-related group (Dataset 2).

Gene Ontology (GO) and InterPro analyses of the broad-sense natto group-specific set (Figures 5, 6, Supplementary Figure 8) indicated an enrichment of DNA-binding proteins, enzymes involved in DNA rearrangement, various metabolic enzymes (hydrolases, transferases), and membrane-associated transporters (Dataset 3, Table 2). The analysis then focused on the natto-related group-specific gene set. The results of the GO analysis for the Biological Process (BP), Molecular Function (MF), and Cellular Component (CC) categories for this set are shown in Supplementary Figures 9, 10, and 11, respectively, with detailed annotations provided in Dataset 4. This analysis revealed that the natto-related group possesses its own distinct set of DNA-binding proteins, various metabolic enzymes with hydrolase or transferase activity, and membrane-localized transport enzymes. A selection of characteristic genes from this set is provided in Table 3.

We performed a simple sensitivity analysis to assess the impact of the chosen threshold for defining nearly group-specific genes. Altering the threshold (to 70%/30% or 90%/10%) predictably changed the total number of genes identified (Datasets 5, 6, 7, 8, 9, 10, 11, and 12). However, the major functional categories enriched in the resulting gene sets for both the broad-sense natto group and the natto-related group remained largely consistent, confirming the robustness of our functional interpretation based on the 80%/20% threshold.

Analysis of particularly interesting genes revealed the following: "broad-sense natto group" strains typically possess two highly similar copies of *rocB* (arginine degradation)[34] and *yveA* (aspartate-proton symporter)[35,36], whereas the "natto-related group" strains contain only one. This group also possesses a duplicate copy of *yesN*, a two-component system response regulator[37]. The *amyE* gene (alpha-amylase)[38] also showed duplication in most "narrow-sense natto group" strains, though the bekang isolate (Food_IND_1) contained only a single copy. The *bglF* homolog (transport of β-glucosides)[39] in the "broad-sense natto group" is significantly longer (609 amino acids) than the version in the "natto-related group" (461 amino acids). In contrast, the *bglH* (degradation of β-glucosides)[39] and *bioF* (biotin synthesis)[18,40] genes in the "broad-sense natto group" are notably shorter, truncated versions compared to the full-length homologs found in the "natto-related group". Among the results for the natto-related group-specific gene set, two genes are of particular interest: *pelB* (Pectate lyase)[41] and *sigV* (sigma factor V)[42]. For *pelB*, no highly similar sequences were detected in the broad-sense natto group. Furthermore, the *pelB* gene exhibited remarkable diversity even within the natto-related group itself. Only the homolog from the kinema-producing *B. subtilis* strain (Food_IND_2) appeared to be full-length, encoding a protein of 304 amino acids. In contrast, the versions found in other natto-related group strains were considerably shorter, ranging from 166 to 170 amino acids, suggesting that they are either truncated or functionally distinct. The other gene

of interest, *sigV*, exhibited copy number variation, with natto-related group strains typically possessing two copies while broad-sense natto group strains have only one.

The loss of function in the flagellar gene *fliF,* previously noted as a characteristic of *B. subtilis* var. *natto*[18], was observed in "narrow-sense natto group" strains but not in the bekang isolate, indicating it is not a universal trait of the "broad-sense natto group". Finally, the gene presence/absence analysis revealed no differences between the "broad-sense natto group" and the "natto-related group" for the key genes associated with polyglutamic acid (PGA) synthesis (*pgsBCA*) or its main regulators[3]. Furthermore, the synteny of the genomic region containing these PGA-related genes was found to be highly conserved across all analyzed strains. This finding is consistent with previous comparative study[18], which also failed to identify clear differences within the PGA synthesis operon itself that could explain the phenotypic variations in PGA production between natto and related strains.

Discussion

In this study, we present a compelling case study of a single *B. subtilis* strain from Indian bekang (Food_IND_1) that exhibits a striking accessory gene similarity to the phylogenetically distant Japanese *B. subtilis* var. *natto* clade ("narrow-sense natto group"). This core finding highlights a discrepancy between systematic relatedness (based on core genes) and functional similarity (based on accessory genes) at the boundary of the natto clade. Our quantitative analysis using Jaccard distance clearly positioned the bekang strain as the functional nearest neighbor to the narrow-sense natto group, while the systematic nearest neighbor from Nepal (Food_NPL_1) was functionally more distant (Figure 2). This finding is particularly intriguing given that a defining characteristic of Japanese natto is its intense PGA-derived viscosity—a feature that distinguishes it from most other *B. subtilis*-fermented soybean products. As noted in the Introduction, bekang is also reported to be a highly viscous and stringy product[7]. Bekang is a traditional food consumed not only in Mizoram, India, but also in the adjacent Chin State of Myanmar. The shared genomic profile leads to the hypothesis that this specific bekang-producing lineage may also possess a notable capacity for PGA production. Indeed, a previous study reported substantial PGA production in other bekang-isolated strains, supporting this hypothesis[7]. Although the strains analyzed in that study were different from Food_IND_1, the potential for high PGA production presents a compelling candidate for the key functional trait linked to the conserved accessory gene repertoire ("broad-sense natto group" signature) we observed.

How did the Food_IND_1 strain come to share an adaptive module with distant natto strains? We propose two competing, and equally plausible, evolutionary scenarios. The first hypothesis is horizontal gene transfer (HGT)[43]. We propose that a "natto-type" adaptive module—a large, co-evolved set of genes conferring advantageous traits for soybean fermentation—was transferred as a "plug-and-play" system, allowing for rapid adaptation to the soybean niche[44]. This is plausible, as

B. subtilis is known for its natural competence[45]. Our network analysis, which detected genetic exchange between the bekang strain and a Myanmar strain, suggests this lineage may be part of a broader network of gene flow. The alternative hypothesis involves selective retention of ancestral traits and differential gene loss[46,47]. This scenario posits that a common ancestor of both the "narrow-sense natto group" and the "natto-related group" possessed this "soybean-adaptation" gene set. Subsequently, this module was lost in most "natto-related" lineages (like the Nepalese strain) but was selectively retained in both the bekang and natto lineages due to similar selective pressures encountered in viscous soybean fermentation niches. At present, our data do not allow us to definitively distinguish between these two scenarios. Both remain viable explanations for the observed genomic paradox.

Our analysis also highlighted the remarkable genetic homogeneity among the Japanese *B. subtilis* var. *natto* strains (the "narrow-sense natto group"). This is likely attributable to the modern industrial practice of using a limited number of elite starter cultures (spores) selected for high PGA productivity[4], a practice that imposes low evolutionary pressure during fermentation and creates an artificial bottleneck. However, the presence of phylogenetically similar strains within this group isolated from natural environments (e.g., the deep-sea isolate Env_JPN_1[12]) suggests the lineage is not purely an industrial artifact. This might be explained by the "escape" of resilient industrial spores back into diverse ecosystems, or potentially that the lineage was already naturally homogeneous before widespread industrialization.

The distribution of food-derived (Food) and environmental (Env) strains within our focused 42-strain dataset presents a complex picture that resists simple interpretation regarding selective pressures. The "natto-related group" (n=16) consists entirely of food isolates, reflecting the study's focus on strains from fermented foods that are phylogenetically close to the natto clade. Conversely, the highly homogeneous "narrow-sense natto group" (n=26) itself contains strains isolated from

environmental sources (e.g., Env_JPN_1). The origin and history of these environmental strains clustering within the core natto clade are unknown; they could represent strains escaped from industrial settings, strains from natural populations closely related to those used industrially, or other scenarios. Given these significant uncertainties, it is difficult to definitively conclude how food fermentation history versus natural environmental pressures have shaped the observed genomic patterns based solely on the Food/Env labels. What remains clear, however, is the existence of the conserved "natto-type" accessory gene module. Its presence in both the core natto clade (with its mix of Food and Env isolates) and the phylogenetically distant, food-derived bekang isolate suggests this adaptive toolkit is not merely a product of modern industrial selection but represents a pre-existing, successful strategy for utilizing soybean substrates.

These findings strongly support a model of polygenic adaptation, in which characteristic traits such as efficient soybean substrate utilization are not dictated by a single gene but by a large, conserved set of accessory genes acting in concert. The "broad-sense natto group"-specific gene set represents one such successful polygenic module.

Finally, this study has several primary limitations. First, and most critically, our central finding regarding the natto-bekang connection is based on the genomic analysis of a single bekang isolate (n=1). Future studies involving the genomic analysis of a broader collection of *B. subtilis* strains from bekang are crucial to determine whether the conserved accessory repertoire we observed in Food_IND_1 is a common feature. Furthermore, this investigation should be extended to the diverse *B. subtilis* strains from Myanmar's fermented soybean foods. The Bamar people of Myanmar represent another major population—alongside the Japanese and Koreans—with a rich tradition of producing *B. subtilis*-fermented soybean foods, making the region a critical and largely unexplored nexus for this bacterium's diversity. Our discovery of genetic exchange between the Indian bekang and Myanmar pe poke strains further underscores the importance of this region. Such expanded

research will be essential to map the complex pathways of gene flow and understand the adaptive radiation of these bacteria across Asia. Second, our study is based on *in silico* genomic data. We have identified a set of candidate genes, but we have not shown that they are actively expressed. Future work, such as transcriptomics, is essential to confirm whether these genes are truly being expressed during soybean fermentation and contribute to the adaptive phenotype. A further limitation is that many genomes used were draft assemblies. This makes the reliable analysis of repetitive sequences like IS elements, which are known to be abundant in natto strains and act as important evolutionary drivers, technically challenging. This remains an important avenue for future research using complete genomes.

Methods

Genome Data Acquisition and Quality Control

The 55 *B. subtilis* strains used in this study are detailed in Table 1. This initial set was selected to explore the diversity surrounding *B. subtilis* var. *natto*, including strains identified through sequence similarity searches using *B. subtilis* var. *natto* sequences as queries and from relevant literature. The key bekang isolate (Food_IND_1, Miz-8) was not a culture collection strain, but was reported as being directly isolated from traditional bekang in Mizoram, India[6]. For genomes where assemblies were not publicly available, raw reads were retrieved from public read archives and assembled de novo using SPAdes (version 4.2.0)[48]. Assembled contigs shorter than 201 bp were subsequently removed using the seq -m 201 option in SeqKit (version 2.8.2)[49]. The quality of all genome sequences was assessed by calculating completeness and contamination values using CheckM2 (version 1.1.0)[50]. To ensure consistent annotation across all datasets, all genome sequences were re-annotated using Prokka (version 1.14.6)[51]. The resulting GFF, GenBank, and FAA files are available from https://drive.google.com/file/d/1dRA0wjLvmyoJHyVJF8F1l4Pl5rchX7GS/view.

Pangenome and Phylogenetic Analysis

Using the GFF files generated by Prokka as input, a pangenome analysis was conducted with Roary (version 3.13.0)[31] using the options -e -n -v -r. The resulting gene presence/absence matrices for both the full set of 55 samples (gene_presence_absence_55_samples.csv) and the subset of 42 samples (gene_presence_absence_42_samples.csv) can be accessed at https://drive.google.com/file/d/1dRA0wjLvmyoJHyVJF8F1l4Pl5rchX7GS/view. Core-gene phylogenetic trees were constructed from the core_gene_alignment_55_samples.aln and core_gene_alignment_42_samples.aln files (available from https://drive.google.com/file/d/1dRA0wjLvmyoJHyVJF8F1l4Pl5rchX7GS/view) generated by

Roary. For building a maximum-likelihood phylogenetic tree, IQ-TREE 2 (version 2.2.2.3)[52] was used with the options -m MFP -bb 1000 -alrt 1000. The -m MFP option enables automatic substitution model selection. The best-fit substitution model, as determined by ModelFinder under the Bayesian Information Criterion (BIC), was GTR+F+I+R5 for the 55-strain analysis and GTR+F+I+R2 for the 42-strain analysis. The resulting phylogenetic tree, including support values, was visualized using FigTree (version 1.4.4) (http://tree.bio.ed.ac.uk/software/figtree/). To generate a figure that merges the phylogenetic tree with the gene presence/absence matrix (Supplementary Figure 2), we used a modified version of the roary_plots.py script, which is provided at https://github.com/sanger-pathogens/Roary.git. This modified script, roary_plots_2.py (Dataset 13), takes the treefile from IQ-TREE 2 and the gene_presence_absence.csv file from Roary as input. The primary modification to this script was the implementation of midpoint rooting for the phylogenetic tree.

Cluster Analysis Based on Gene Presence/Absence Profiles

To perform cluster analysis based on functional profiles, the gene_presence_absence.csv files generated by Roary (gene_presence_absence_55_samples.csv for the 55-strain analysis and gene_presence_absence_42_samples.csv for the 42-strain analysis) were directly analyzed using a custom Python script, one_step_cluster.py (Dataset 13). This script calculates pairwise distance matrices using several metrics, including Jaccard, Sørensen-Dice, Hamming, and Euclidean distances. For this study, we selected the Jaccard distance metric, as it appropriately ignores joint absences ("double zeros") in binary presence/absence data. Based on the calculated Jaccard distance matrices for both the 55 strains and the focused 42 strains, the one_step_cluster.py script performed hierarchical clustering and generated the resulting heatmaps and dendrograms. This analysis was

employed as a quantitative and exploratory map to assess functional similarity, rather than to define statistically discrete groups.

Visualization of Synteny Blocks

To visualize synteny blocks among the three selected chromosome-level genomes, Easyfig (version 2.25)[53] was used. This analysis required three GenBank annotation files and two BLAST[54] comparison files as input. The annotation files were the GenBank-formatted outputs generated by Prokka. The two required BLAST files were generated from sequential pairwise blastn searches: the first search compared genome 1 (query) against genome 2 (database), and the second compared genome 2 (query) against genome 3 (database). For both searches, the output was specified in tabular format using the -outfmt 6 option. Using these three GenBank files and two BLAST files as input, Easyfig was run with its default parameters to generate the comparative visualization.

Phylogenetic Network Analysis

A phylogenetic network was constructed from the core gene alignment to investigate potential reticulate evolutionary events, such as recombination. The analysis was performed using SplitsTree (version 6.4.16)[55] with default settings. The input file was the core_gene_alignment_42_samples.aln or core_gene_alignment_55_samples.aln generated by Roary, which was renamed with a .fasta file extension prior to the analysis.

Identification and Extraction of Group-Specific Accessory Genes

For the identification of "broad-sense natto group"-specific and "natto-related group"-specific genes, "nearly group-specific genes" were first defined using a criterion of ≥80% presence within the target group and ≤20% presence in the comparison group. Alternative thresholds, such as 70%/30%

and 90%/10%, were also evaluated to assess the robustness of the findings. The analysis was performed on the gene_presence_absence_42_samples.csv file from the 42-strain Roary analysis (comprising the "narrow-sense natto group", the bekang strain, and the "natto-related group"). Custom scripts, analyze_genes_A_specific.py and analyze_genes_B_specific.py (Dataset 13), were executed to parse this file and extract the names of all genes that met the defined criteria for the "broad-sense natto group" and "natto-related group", respectively. The resulting tabular output was then processed with another custom script, process_csv.py (Dataset 13), to create a list containing only the primary gene names from the leftmost column. Finally, a third script, process_fasta.py (Dataset 13), utilized this list of gene names to retrieve the corresponding amino acid sequences in FASTA format from the multiple per-sample protein files (.faa) that were generated by Roary and stored in a specified directory.

Functional Annotation

Functional annotation of the "broad-sense natto group"-specific and "natto-related group"-specific protein sets (.faa files) was performed using OmicsBox (version 3.4.6; GO version March 16, 2025). The workflow consisted of several integrated steps. First, a similarity search was conducted against the Diamond BLAST database (2024-11-20 release) using the blastp mode[56]. This search was taxonomically filtered to *Bacillus* (taxid: 1386) with an E-value cutoff of 1.0E-3. Next, protein domains and families were identified by running InterProScan (version 5.72-103.0)[57]. Finally, GO terms were mapped and assigned to each sequence within OmicsBox based on the combined results of the previous steps[58,59,60]. For the final annotation, results were filtered with an E-value-Hit Filter of 1.0E-6 and a Hit Filter of 500.

Use of Generative AI

The generative AI models Gemini and ChatGPT were used to improve the language and clarity of the manuscript and to assist in writing the Python scripts.

References

1. Harahap, I. A., Suliburska, J., Karaca, A. C., Capanoglu, E. & Esatbeyoglu, T. Fermented soy products: a review of bioactives for health from fermentation to functionality. *Compr. Rev. Food Sci. Food Saf.* **24**, e70080; 10.1111/1541-4337.70080 (2025).
2. Gopikrishna, T., Suresh Kumar, H. K., Perumal, K. & Elangovan, E. Impact of *Bacillus* in fermented soybean foods on human health. *Ann. Microbiol.* **71**, 1–16 (2021).
3. Elbanna, K., Alsulami, F. S., Neyaz, L. A. & Abulreesh, H. H. Poly-γ-glutamic acid: a unique microbial biopolymer with diverse commercial applicability. *Front. Microbiol.* **15,** 1348411; 10.3389/fmicb.2024.1348411 (2024).
4. Miyazawa, T. et al. Biological functions of compounds from *Bacillus subtilis* and its subspecies, *Bacillus subtilis* natto. *Food Bioengineering* **1**, 241–251 (2022).
5. Kim, I. S., Hwang, C. W., Yang, W. S. & Kim, C. H. Current perspectives on the physiological activities of fermented soybean-derived cheonggukjang. *Int. J. Mol. Sci.* **22**, 5746; 10.3390/ijms22115746 (2021).
6. Kumar, H. K. S., Gopikrishna, T., Tapasya, K., Perumal, K. & Elavarashi, E. A computational genome analysis of strain *Bacillus subtilis* MIZ-8 isolated from bekang reveals a distinct chromosome and plasmid conferring selective advantage. *J. Microbiol. Biotechnol. Food Sci.* **13,** e9141; 10.55251/jmbfs.9141 (2023).
7. Chettri, R. & Tamang, J. P. Functional properties of Tungrymbai and Bekang, naturally fermented soybean foods of North East India. *J. Ethn. Foods* **1,** 8–14 (2014).
8. Tani, T. et al. A case of community-acquired pneumonia caused by *Bacillus subtilis* subsp. *natto* in an immunocompetent patient. *Respirol. Case Rep.* **12**, e01384; 10.1002/rcr2.1384 (2024).

9. Tan, S., Meng., Y, Su., A, Zhang., C & Ren, Y. Draft genome sequence of *Bacillus subtilis* subsp. *natto* strain CGMCC 2108, a high producer of poly-γ-glutamic acid. *Genome Announc.* **4**, e00510-16; 10.1128/genomea.00426-16 (2016).
10. Wang, F., Gong, L., Zhou, L. & Liang, J. Complete genome sequence of the poly-γ-glutamate-synthesizing bacterium *Bacillus subtilis* Bs-115. *Genome Announc.* **6**, e00318-18; 10.1128/genomea.00197-18 (2018).
11. Dong, H., Chang, J., He, X., Hou, Q. & Long, W. Complete genome sequence of *Bacillus subtilis* strain CGMCC 12426, an efficient poly-γ-glutamate producer. *Genome Announc.* **5**, e01168-17; 10.1128/genomea.01163-17 (2017).
12. Wei, Y., Cao, J., Fang, J., Kato, C. & Cui, W. Complete genome sequence of *Bacillus subtilis* strain 29R7-12, a piezophilic bacterium isolated from coal-bearing sediment 2.4 kilometers below the seafloor. *Genome Announc.* **5**, e01728-16; 10.1128/genomea.01621-16 (2017).
13. Min, X. et al. Comparative transcriptome analysis reveals the underlying mechanism for over-accumulation of menaquinone-7 in *Bacillus subtilis* natto mutant. *Biochem*. *Eng*. *J.* **174**, 108097; 10.1016/j.bej.2021.108097 (2021).
14. Dikson, D. *et al.* Whole-genome analysis of *Bacillus subtilis* G8 isolated from natto. *Biodivers. J. Biol. Divers.* **23,** 1378–1385 (2022).
15. Zhu, J. *et al.* Genomic characterization and related functional genes of γ-polyglutamic acid producing *Bacillus subtilis*. *BMC Microbiol.* **24,** 125; 10.1186/s12866-024-03262-z (2024).
16. Kamada, M. *et al.* Whole genome complete resequencing of *Bacillus subtilis* natto by combining long reads with high-quality short reads. *PLoS ONE* **9,** e109999; 10.1371/journal.pone.0109999 (2014).

17. Kubo, Y. *et al.* Complete genome sequence of *Bacillus subtilis* subsp. *natto* NARUSE using PacBio sequencing. *Microbiol. Resour. Announc.* **12,** e00578-23; 10.1128/MRA.00578-23 (2023).

18. Kamada, M. *et al.* Whole-genome sequencing and comparative genome analysis of *Bacillus subtilis* strains isolated from non-salted fermented soybean foods. *PLoS ONE* **10,** e0141369; 10.1371/journal.pone.0141369 (2015).

19. Parks, D. *et al.* Genome sequence of *Bacillus subtilis* natto VK161, a novel strain that produces vitamin K2. *Microbiol. Resour. Announc.* **8,** e00854-19; 10.1128/mra.00444-19 (2019).

20. Tamang, J. P., Kharnaior, P. & Pariyar, P. Whole genome sequencing of the poly-γ-glutamic acid-producing novel *Bacillus subtilis* Tamang strain, isolated from spontaneously fermented kinema. *Food Res. Int.* **190,** 114655; 10.1016/j.foodres.2024.114655 (2024).

21. Bang, M. S. *et al.* Complete genome sequence of *Bacillus subtilis* strain DKU_NT_02, isolated from traditional Korean food using soybean (chung-gook-jang) for high-quality poly-γ-glutamic acid activity. *Genome Announc.* **6,** e00525-18; 10.1128/genomea.00525-18 (2018).

22. Jeong, H. W. *et al.* Complete genome sequence of *Bacillus subtilis* strain DKU_NT_03, isolated from a traditional Korean food using soybean (Chung-gook-jang) for high-quality nattokinase activity. *Genome Announc*. **6,** e00526-18; 10.1128/genomea.00526-18 (2018).

23. Choi, J. W. *et al.* Engineering *Bacillus subtilis* J46 for efficient utilization of galactose through adaptive laboratory evolution. *AMB Express* **14,** 14; 10.1128/genomea.00526-18 (2024).

24. Kunst, F. J. *et al.* The complete genome sequence of the gram-positive bacterium *Bacillus subtilis*. *Nature* **390,** 249–256 (1997).

25. Choubane, S., Gabed, N., Khelil, O. & Cheba, B. A. Draft genome sequence of *Bacillus subtilis* TLO3, isolated from olive tree rhizosphere soil. *Microbiol. Resour. Announc.* **7,** e01128-18; 10.1128/mra.00852-18 (2018).

26. Hamdy, A. A. *et al.* Complete genome sequence and comparative analysis of two potential probiotics *Bacillus subtilis* isolated from honey and honeybee microbiomes. *J. Genet. Eng. Biotechnol.* **18,** 34; 10.1186/s43141-020-00050-w (2020).

27. Pramod, S. *et al.* Data on the genome of *Bacillus subtilis* A1-Midalam from beach soil. *Data Brief* **39,** 107552; 10.1016/j.dib.2021.107552 (2021).

28. Epparti, P., Eligar, S. M., Sattur, A. P., Kumar, B. G. & Halami, P. M. Characterization of dual bacteriocins producing *Bacillus subtilis* SC3.7 isolated from fermented food. *LWT* **154,** 112854; 10.1016/j.lwt.2021.112854 (2022).

29. Golicz, A. G., Bayer, P. E., Bhalla, P. L., Batley, J. & Edwards, D. Computational pan-genomics: status, promises and challenges. *Brief. Bioinform.* **21,** 1–19 (2020).

30. Verma, D., Satyanarayana, T. & Dias, P. J. Microbial comparative genomics and pangenomics: new tools, approaches and insights into gene and genome evolution. *Front. Genet.* **15,** 1490645; 10.3389/fgene.2024.1490645 (2024).

31. Page, A. J. *et al.* Roary: rapid large-scale prokaryote pan genome analysis. *Bioinformatics* **31,** 3691–3693 (2015).

32. Sutton, G. *et al.* A pan-genome method to determine core regions of the *Bacillus subtilis* and *Escherichia coli* genomes. *F1000Research*, **10,** 286; 10.12688/f1000research.51873.2 (2021).

33. Saikat, T. A., Khan, M. A. S., Islam, M. S., Tasnim, Z., & Ahmed, S. Characterization and genome mining of *Bacillus subtilis* BDSA1 isolated from river water in Bangladesh: A promising bacterium with diverse biotechnological applications. *Heliyon*, **10,** e34369; 10.1016/j.heliyon.2024.e34369 (2024).

34. Warneke, R. *et al.* Ornithine is the central intermediate in the arginine degradative pathway and its regulation in *Bacillus subtilis*. *J. Biol. Chem.* **299,** 104944; 10.1016/j.jbc.2023.104944 (2023).

35. Lorca, G., Winnen, B. & Saier, M. H. Jr. Identification of the L-aspartate transporter in *Bacillus subtilis*. *J. Bacteriol.* **185,** 3218–3222 (2003).

36. Zaprasis, A., Bleisteiner, M., Kerres, A., Hoffmann, T. & Bremer, E. Uptake of amino acids and their metabolic conversion into the compatible solute proline confers osmoprotection to *Bacillus subtilis*. *Appl. Environ. Microbiol.* **81,** 250–259 (2015).

37. Poncet, S., Soret, M., Mervelet, P., Deutscher, J., & Noirot, P. Transcriptional activator YesS is stimulated by histidine-phosphorylated HPr of the *Bacillus subtilis* phosphotransferase system. *J. Biol. Chem.* **284,** 28188–28197(2009).

38. Murphy, N., McConnell, D. J. & Cantwell, B. A. The DNA sequence of the gene and genetic control sites for the excreted *B. subtilis* enzyme β-glucanase. *Nucleic Acids Res.* **12,** 5355–5367 (1984).

39. Le Coq, D., Lindner, C., Krüger, S., Steinmetz, M. & Stülke, J. New β-glucoside (*bgl*) genes in *Bacillus subtilis*: the *bglP* gene product has both transport and regulatory functions similar to those of BglF, its *Escherichia coli* homolog. *J. Bacteriol.* **177,** 1527–1535 (1995).

40. Sasaki, M., Kawamura, F. & Kurusu, Y. Genetic analysis of an incomplete *bio* operon in a biotin auxotrophic strain of *Bacillus subtilis* natto OK2. *Biosci. Biotechnol. Biochem.* **68,** 739–742 (2004).

41. Nasser, W., Awade, A. C., Reverchon, S. & Robert-Baudouy, J. Pectate lyase from *Bacillus subtilis*: molecular characterization of the gene, and properties of the cloned enzyme. *FEBS Lett.* **335,** 319–326 (1993).

42. Ho, T. D., Hastie, J. L., Intile, P. J. & Ellermeier, C. D. The *Bacillus subtilis* extracytoplasmic function σ factor σV is induced by lysozyme and provides resistance to lysozyme. *J. Bacteriol.* **193,** 6215–6222 (2011).

43. Arnold, B. J., Huang, I. T. & Hanage, W. P. Horizontal gene transfer and adaptive evolution in bacteria. *Nat. Rev. Microbiol.* **20,** 206–218 (2022).

44. Good, B. H., Bhatt, A. S. & McDonald, M. J. Unraveling the tempo and mode of horizontal gene transfer in bacteria. *Trends Microbiol*. **32,** 52–64 (2024).

45. Spizizen, J. Transformation of biochemically deficient strains of *Bacillus subtilis* by deoxyribonucleate. *Proc. Natl. Acad. Sci. U. S. A.* **44,** 1072–1078 (1958).

46. Albalat, R. & Cañestro, C. Evolution by gene loss. *Nat. Rev. Genet.* **17,** 379–391 (2016).

47. Mira, A., Ochman, H. & Moran, N. A. Deletional bias and the evolution of bacterial genomes. *Trends Genet.* **17,** 589–596 (2001).

48. Prjibelski, A., Antipov, D., Meleshko, D., Lapidus, A. & Korobeynikov, A. Using SPAdes de novo assembler. *Curr. Protoc. Bioinformatics* **70,** e102; 10.1002/cpbi.102 (2020).

49. Shen, W., Le, S., Li, Y. & Hu, F. SeqKit: a cross-platform and ultrafast toolkit for FASTA/Q file manipulation. *PLoS ONE* **11,** e0163962; 10.1371/journal.pone.0163962 (2016).

50. Chklovski, A., Parks, D. H., Woodcroft, B. J. & Tyson, G. W. CheckM2: a rapid, scalable and accurate tool for assessing microbial genome quality using machine learning. *Nat. Methods* **20,** 1203–1212 (2023).

51. Seemann, T. Prokka: rapid prokaryotic genome annotation. *Bioinformatics* **30,** 2068–2069 (2014).

52. Minh, B. Q. *et al.* IQ-TREE 2: new models and efficient methods for phylogenetic inference in the genomic era. *Mol. Biol. Evol.* **37,** 1530–1534 (2020).

53. Sullivan, M. J., Petty, N. K. & Beatson, S. A. Easyfig: a genome comparison visualizer. *Bioinformatics* **27,** 1009–1010 (2011).

54. Camacho, C. *et al.* BLAST+: architecture and applications. *BMC Bioinformatics* **10,** 421 (2009).

55. Huson, D. H. & Bryant, D. The SplitsTree app: interactive analysis and visualization using phylogenetic trees and networks. *Nat. Methods* **21**, 1773–1774 (2024).

56. Buchfink, B., Reuter, K. & Drost, H. G. Sensitive protein alignments at tree-of-life scale using DIAMOND. *Nat. Methods* **18,** 366–368 (2021).

57. Jones, P. *et al.* InterProScan 5: genome-scale protein function classification. *Bioinformatics* **30,** 1236–1240 (2014).

58. Ashburner, M. *et al.* Gene ontology: tool for the unification of biology. *Nat. Genet.* **25,** 25–29 (2000).

59. The UniProt Consortium. UniProt: the Universal Protein Knowledgebase in 2023. *Nucleic Acids Res.* **51,** D523–D531 (2023).

60. Götz, S. *et al.* High-throughput functional annotation and data mining with the Blast2GO suite. *Nucleic Acids Res.* **36,** 3420–3435 (2008).

Acknowledgements

We are especially grateful to Dr. Myat Htoo San of the National Institute of Advanced Industrial Science and Technology (AIST), Hokkaido, Japan, and her friend, Ms. Zing Cin Tial, a member of the Chin community from Hakha, Chin State, Myanmar. They kindly provided valuable information and cultural insights into the traditional production of bekang in Chin State, Myanmar, for which there is little published literature. We also thank Drs. Taiki Futagami and Hisanori Tamaki of the Faculty of Agriculture, Kagoshima University, and Drs. Masatoshi Goto and Genta Kobayashi of the Faculty of Agriculture, Saga University, for guiding us into the research of fermented foods.

Funding

This study was supported in part by the Institute for Fermentation, Osaka, Japan (IFO).

Author Contributions

K.S. and Y.N. conceived and designed the study, performed the bioinformatic analyses, and interpreted the data. Y.N. wrote the original manuscript draft, and K.S. reviewed and edited the manuscript. Both authors read and approved the final manuscript.

Data Availability Statement

The primary genome sequence data analyzed in this study were retrieved from publicly available databases; specific accession numbers for all strains are detailed in Table 1. The key data files generated during the computational analysis, including the gene presence/absence matrices, can be accessed at https://drive.google.com/file/d/1dRA0wjLvmyoJHyVJF8F1l4Pl5rchX7GS/view. All custom Python scripts developed for this work are available as Dataset 13.

Competing Interests

Kiyohiko Seki and Yukio Nagano conduct collaborative research with Marumiya, Inc., a food manufacturer that produces natto. Yukio Nagano also conducts collaborative research with Senoo Suisan, Inc., and Sante Laboratories, Inc. In addition, he is a founding member of Smart Review Technologies Co., Ltd., which is currently being established. The authors declare that these collaborations are entirely separate from the present study. Specifically, the collaborative research with Marumiya concerns different aspects of natto production and had no role in the study design, data collection and analysis, decision to publish, or preparation of this manuscript.

Figure Legends

Figure 1. Core-genome-based phylogeny and accessory gene presence/absence matrix of the 42 *B. subtilis* strains. The phylogenetic tree on the left was constructed from a core genome alignment of 42 strains using the maximum likelihood method and is presented as midpoint-rooted. The matrix on the right, generated by Roary, visualizes the pangenome, which consists of 6,762 gene clusters. Each row corresponds to a strain in the tree, and each column represents a single gene cluster. Dark blue cells indicate the presence of a gene cluster in a strain, while white cells indicate its absence. The "narrow-sense natto group" (n=26) is indicated by an orange line. Key strains discussed in the text, the systematic nearest neighbor (Food_NPL_1) and the functional nearest neighbor (Food_IND_1), are highlighted with green squares on their labels.

Figure 2. Hierarchical clustering of 42 *B. subtilis* strains based on accessory gene profiles. The heatmap shows the pairwise shared gene counts between all 42 strains. Hierarchical clustering was performed using Jaccard distance calculated from the binary presence/absence matrix. The "narrow-sense natto group" (n=26) and the "broad-sense natto group" (n=27) are indicated by orange lines. Key strains discussed in the text, the systematic nearest neighbor (Food_NPL_1) and the functional nearest neighbor (Food_IND_1), are highlighted with green squares on their labels.

Figure 3. Chromosome-wide synteny analysis of representative strains. This visualization compares the complete chromosome sequences of three strains, represented by horizontal bars: *B. subtilis* var. *natto* BEST195 (Food_JPN_7, top bar), the bekang isolate (Food_IND_1, middle bar), and *B. subtilis* HRBS-10TDI13 (Food_KOR_9, bottom bar). The shaded regions connecting the genomes denote areas of nucleotide similarity identified by BLASTn, with the grayscale intensity corresponding to the percentage identity shown in the scale bar. The top panel shows the pairwise

comparison between the natto strain (Food_JPN_7) and the bekang isolate (Food_IND_1). The bottom panel shows the pairwise comparison between the bekang isolate (Food_IND_1) and the "natto-related group" strain (Food_KOR_9).

Figure 4. Phylogenetic network of 42 *B. subtilis* strains. The network was constructed from the core genome alignment using the Neighbor-Net algorithm. The tree-like portions of the network depict vertical, clonal inheritance, while the reticulate (box-like) structures indicate conflicting phylogenetic signals suggestive of recombination or horizontal gene transfer events.

Figure 5. Gene Ontology (GO) enrichment analysis f for the "broad-sense natto group"-specific gene set. The figure shows a Directed Acyclic Graph of enriched GO terms, generated using OmicsBox. Each node (box) represents a GO term and displays its ID, description, NodeScore, and the number of associated gene sequences. The color intensity of each node is proportional to its enrichment significance, with more significantly enriched terms shown in shades of orange. The connecting lines represent hierarchical relationships between the terms.

Figure 6. Gene Ontology (GO) enrichment analysis for the "broad-sense natto group"-specific gene set. The figure shows a Directed Acyclic Graph of enriched GO terms. Each box represents a GO term, displaying its ID, description, and the number of associated gene sequences. The color intensity of the boxes is proportional to the significance of enrichment, with more significant terms shown in shades of orange. The connecting lines represent hierarchical relationships between the terms.

615 **Table 1.** Details of the publicly available data used in this study.

Name	Group[a]	Accession number	Strain name	Origin details	Location	Publication
Clin_JPN_1	N	GCF_037094835.1	TUM22925	Patient blood	Japan	8
Clin_JPN_2	N	GCF_037094855.1	TUM22926	Patient bronchoalveolar lavage fluid	Japan	8
Clin_JPN_3	N	GCF_037095795.1	TUM22927	The natto with the patient usually eating	Japan	8
Coll_1	N	GCF_002982175.1	ATCC 21228	N/A	N/A	N/A
Coll_2	N	GCF_024508195.1	BGSC 27E1	N/A	N/A	N/A
Coll_3	N	GCF_001565875.1	CGMCC 2108	Soil	N/A	9
Coll_4	N	GCF_024507815.1	BGSC 27E3	N/A	N/A	N/A
Env_CHN_1	N	GCF_002096095.1	Bs-115	Soil of a corn field	Shandong, China	10
Env_CHN_2	N	GCF_045343855.1	G01	N/A	Guangdong, China	N/A
Env_CHN_3	N	GCF_001890405.1	KH2	Soil	Tianjin, China	11
Env_CHN_4	N	GCF_023278545.1	ZHX3	Activated sludge	Changsha, China	N/A
Env_JPN_1	N	GCF_001902555.1	29R7-12	Coal Bed	Shimokita Peninsula, Japan	12
Food_CHN_1	N	GCF_022701095.1	BN0	Soybean product	Wuxi, China	13
Food_CHN_2	N	GCF_020773035.1	SCP010-1	Bean Paste	Sichuan, China	N/A
Food_IDN_1	N	GCF_027923485.1	G8	Natto	Indonesia	14
Food_JPN_1	N	GCF_003665335.1	N1-1	Natto	Japan	N/A
Food_JPN_2	N	GCF_003665315.1	N2-2	Natto	Japan	N/A
Food_JPN_3	N	GCF_003665355.1	N3-1	Natto	Japan	N/A
Food_JPN_4	N	GCF_033412715.1	N3378-2at	Natto	Hokkaido, Japan	15
Food_JPN_5	N	GCF_033413615.1	N3378-3At	Natto	Hokkaido, Japan	15
Food_JPN_6	N	GCF_003665295.1	N4-2	Natto	Japan	N/A
Food_JPN_7	N	GCF_000209795.2	BEST195	Natto	Japan	16
Food_JPN_8	N	GCF_030297075.1	NARUSE	Natto	Japan	17
Food_JPN_9	N	Assembled from DRR029699[*]	TAKAHASHI	Natto	Japan	18
Food_KOR_1	N	GCF_014961985.1	CMIN-4	Cheonggukjang	Jeonbuk, South Korea	N/A
Food_KOR_2	N	GCF_004323065.1	VK161	Natto	Seongnam, South Korea	19
Food_IND_1	Bekang	GCF_018986855.1	Miz-8	Bekang	Mizoram, India	6
Food_IND_2	R	GCF_037169145.1_	Tamang	Kinema	Sikkim, India	20
Food_KOR_3	R	GCF_003665395.1	2KL1	Cheonggukjang	Jeonju, South Korea	N/A

Food_KOR_4	R	GCF_003665275.1	2RL2-3	Cheonggukjang	Gyeonggi, South Korea	N/A
Food_KOR_5	R	Assembled from DRR029692*	NFRI8338	Cheonggukjang	Seoul, South Korea	18
Food_KOR_6	R	GCF_002269175.1	DKU_NT_02	Cheonggukjang	Cheonan, South Korea	21
Food_KOR_7	R	GCF_002269195.1	DKU_NT_03	Cheonggukjang	Cheonan, South Korea	22
Food_KOR_8	R	GCF_003665195.1	GFR-12	Cheonggukjang	Gyeonggi, South Korea	N/A
Food_KOR_9	R	GCF_001747445.1	HRBS-10TDI13	Doenjang	Sunchang, South Korea	N/A
Food_KOR_10	R	GCF_033113625.1	J46	Doenjang	South Korea	23
Food_KOR_11	R	GCF_046840395.1	KFRI-P74	Fermented soybean paste	Ansung, South Korea	N/A
Food_KOR_12	R	GCF_003665235.1	MH-1	Cheonggukjang	Chungcheongbuk-do, South Korea	N/A
Food_KOR_13	R	GCF_035621695.1_	PN1236	Fermented soybean food	South Korea	N/A
Food_MMR_1	R	Assembled from DRR029694*	NFRI8316	Pe poke	Yangon, Myanmar	18
Food_NPL_1	R	Assembled from DRR029696*	NFRI8292	Kinema	Hille, Nepal	18
Food_THA_1	R	Assembled from DRR029695*	NFRI8347	Thua nao	Chiang Mai, Thailand	18
Coll_5		GCF_000009045.1	168	N/A	N/A	24
Coll_6		GCF_004101945.1	ATCC 11774	N/A	N/A	N/A
Env_DZA_1		GCF_002142595.1	TLO3	Olive tree rhizosphere	Tlemcen, Algeria	25
Env_EGY_1		GCF_009497795.1	MENO2	Honeybee gut	Egypt	26
Env_IND_1		GCF_018454405.1	A1 - Midalam	Beach soil	Tamil Nadu, India	27
Env_USA_1		GCF_037976695.1	FSL K6-1366	HTST Pasteurization	N/A	N/A
Env_USA_2		GCF_047302535.1	SY1483	Root	USA	N/A
Food_BFA_1		GCA_029536855.2	PRO120	Maari	Toulfe, Burkina Faso	N/A
Food_IND_3		GCF_018224865.2	SC3.7	Soybean seed Chutney	Manipur, India	28
Food_KOR_14		GCF_030285965.1	KFRI-FA111	Jeotgal	South Korea	N/A
Food_KOR_15		GCF_003665215.1	PJ-7	Cheonggukjang	Gyeonggi, South Korea	N/A
Food_KOR_16		GCF_009913275.1	SRCM102754	Doenjang	South Korea	N/A
Food_LAO_1		Assembled from DRR029693*	NFRI8302	Thua nao	Ruanpanpan, Laos	18

*Assembled *de novo* from Sequence Read Archive data. Abbreviations used in “Group”: N = "Narrow-sense natto group" (n=26), R = "Natto-related group" (n=15), Bekang = the single Bekang isolate (Food_IND_1). Abbreviations used in “Name”: Clin – Clinical study; Coll – Collection; Env – Environmental; JPN – Japan; CHN – China; IDN – Indonesia; IND – India; KOR – South Korea; MMR – Myanmar; NPL – Nepal; THA – Thailand; DZA – Algeria; EGY – Egypt; BFA – Burkina Faso; LAO – Laos.

619 **Table 2.** A selection of nearly "broad-sense natto group"-specific genes.

SeqName[1]	The number in broad-sense natto group[2]	Presence in Bekang strain (1/0)	The number in Group B	Description[3]	GO IDs	GO Names	Enzyme Codes	Enzyme Names
xerC_6	27	1	2	site-specific integrase	P:GO:0006310; F:GO:0003677	P:DNA recombination; F:DNA binding		
xerC_9	27	1	1	tyrosine-type recombinase/integrase	P:GO:0006310; F:GO:0003677	P:DNA recombination; F:DNA binding		
xerD_2	27	1	2	tyrosine-type recombinase/integrase	P:GO:0006310; F:GO:0003677	P:DNA recombination; F:DNA binding		
xerD_3	27	1	1	site-specific integrase	P:GO:0006310; F:GO:0003677	P:DNA recombination; F:DNA binding		
group_2454	27	1	0	site-specific integrase	P:GO:0006310; F:GO:0003677	P:DNA recombination; F:DNA binding		
group_4906	27	1	3	transposase	P:GO:0006310; F:GO:0003677; F:GO:0140097	P:DNA recombination; F:DNA binding; F:catalytic activity, acting on DNA		
group_6181	22	1	1	IS21 family transposase	P:GO:0006310; F:GO:0003677; F:GO:0140097	P:DNA recombination; F:DNA binding; F:catalytic activity, acting on DNA		
group_1396	25	0	3	helix-turn-helix transcriptional regulator	F:GO:0003677	F:DNA binding		
group_1783	27	1	0	ERCC4 domain-containing protein	F:GO:0003677; F:GO:0003824	F:DNA binding; F:catalytic activity		
group_1787	27	1	1	host-nuclease inhibitor Gam family protein	F:GO:0003677	F:DNA binding		
group_1890	27	1	1	helix-turn-helix transcriptional regulator	F:GO:0003677	F:DNA binding		
group_2132	27	1	2	helix-turn-helix domain-containing protein	F:GO:0003677	F:DNA binding		
group_2184	27	1	2	helix-turn-helix transcriptional	F:GO:0003677	F:DNA binding		

				regulator				
group_2238	27	1	1	helix-turn-helix transcriptional regulator	F:GO:0003677	F:DNA binding		
group_2240	27	1	1	FtsK/SpoIIIE domain-containing protein	F:GO:0003677	F:DNA binding		
group_2450	27	1	0	phage regulatory protein/antirepressor Ant	F:GO:0003677	F:DNA binding		
group_2451	27	1	0	helix-turn-helix transcriptional regulator	F:GO:0003677	F:DNA binding		
group_2452	27	1	0	helix-turn-helix transcriptional regulator	F:GO:0003677	F:DNA binding		
group_2456	27	1	0	helix-turn-helix transcriptional regulator	F:GO:0003677	F:DNA binding		
group_2457	27	1	0	helix-turn-helix domain-containing protein	F:GO:0003677	F:DNA binding		
group_2531	27	1	0	helix-turn-helix transcriptional regulator	F:GO:0003677	F:DNA binding		
group_2546	27	1	3	helix-turn-helix transcriptional regulator	F:GO:0003677	F:DNA binding		
group_2211	27	1	3	MarR family transcriptional regulator	P:GO:0006355; F:GO:0140110	P:regulation of DNA-templated transcription; F:transcription regulator activity		
group_2518	27	1	1	sigma factor-like helix-turn-helix DNA-binding protein	P:GO:0006355; F:GO:0140110	P:regulation of DNA-templated transcription; F:transcription regulator activity		
group_5156	26	1	1	IS3 family transposase	P:GO:0015074; F:GO:0003676	P:DNA integration; F:nucleic acid binding		
insK	23	1	1	IS3 family transposase	P:GO:0015074; F:GO:0003676	P:DNA integration; F:nucleic acid binding		
amyE_1	25	0	3	Alpha-amylase	F:GO:0016787 P:GO:0005975	F:hydrolase activity P:carbohydrate	EC:3.2.1.1	alpha-amylase

						metabolic process		
bglH_2	26	1	3	Aryl-phospho-beta-D-glucosidase BglH	F:GO:0016787 P:GO:0005975	F:hydrolase activity P:carbohydrate metabolic process	EC:3.2.1	Glycosylases
cheC_1	26	1	0	CheY-P phosphatase CheC	F:GO:0016787	F:hydrolase activity	EC:3	Hydrolases
cwlA_2	27	1	1	N-acetylmuramoyl-L-alanine amidase	F:GO:0016787 P:GO:1901135;	F:hydrolase activity P:carbohydrate derivative metabolic process;	EC:3.5.1.28	N-acetylmuramoyl-L-alanine amidase
lagD	27	1	3	peptide cleavage/export ABC transporter	P:GO:0055085; F:GO:0005215; F:GO:0016787; F:GO:0140096; F:GO:0140657	P:transmembrane transport; F:transporter activity; F:hydrolase activity; F:catalytic activity, acting on a protein; F:ATP-dependent activity	EC:3.4; EC:7.6.2.2; EC:7.2.2; EC:3.6.1.15	Acting on peptide bonds (peptidases); ABC-type xenobiotic transporter; Catalysing the translocation of inorganic cations; nucleoside-triphosphate phosphatase
rocB_1	25	1	2	M20/M25/M40 family metallo-hydrolase	F:GO:0016787	F:hydrolase activity	EC:3	Hydrolases
uvrD	22	1	3	ATP-dependent helicase	F:GO:0016787	F:hydrolase activity	EC:3	Hydrolases
yesZ_1	26	0	1	Beta-galactosidase YesZ	F:GO:0016787 P:GO:0005975	F:hydrolase activity P:carbohydrate metabolic process	EC:3.2.1.23	beta-galactosidase
yesZ_2	27	1	1	Beta-galactosidase YesZ	F:GO:0016787 P:GO:0005975	F:hydrolase activity P:carbohydrate metabolic process	EC:3.2.1.23	beta-galactosidase
group_689	27	1	3	ABC transporter ATP-binding protein	P:GO:0055085; F:GO:0005215; F:GO:0016787; F:GO:0140657	P:transmembrane transport; F:transporter activity; F:hydrolase activity; F:ATP-dependent activity	EC:7.2.2; EC:3.6.1.15	Catalysing the translocation of inorganic cations; nucleoside-triphosphate phosphatase
group_2244	27	1	1	N-acetylmuramoyl-L-alanine amidase	F:GO:0016787 P:GO:1901135;	F:hydrolase activity P:carbohydrate derivative metabolic	EC:3.5.1.28	N-acetylmuramoyl-L-alanine amidase

						process;		
group_2498	27	1	1	glucosaminidase domain-containing protein	F:GO:0016787	F:hydrolase activity	EC:3.5.1.4	amidase
group_2439	27	1	2	terminase TerL endonuclease subunit	F:GO:0003824	F:catalytic activity		
bioF	27	1	3	8-amino-7-oxononanoate synthase	P:GO:0006766; P:GO:0006790; F:GO:0016740	P:vitamin metabolic process; P:sulfur compound metabolic process; F:transferase activity	EC:2.3.1.47	8-amino-7-oxononanoate synthase
bglF	27	1	2	PTS beta-glucoside transporter subunit IIABC	P:GO:0055085; F:GO:0005215; F:GO:0016740; C:GO:0005886	P:transmembrane transport; F:transporter activity; F:transferase activity; C:plasma membrane	EC:2.7.1	Transferring phosphorus-containing groups
yheI_2	25	0	2	ABC transporter ATP-binding protein	P:GO:0006790; P:GO:0055085; P:GO:0055086; F:GO:0005215; F:GO:0016740; F:GO:0140657	P:sulfur compound metabolic process; P:transmembrane transport; P:nucleobase-containing small molecule metabolic process; F:transporter activity; F:transferase activity; F:ATP-dependent activity	EC:7.2.2; EC:2.7.1.24	Catalysing the translocation of inorganic cations; dephospho-CoA kinase
group_2412	26	0	2	acyl-CoA carboxylase subunit beta	P:GO:0006629; F:GO:0016740; F:GO:0016874	P:lipid metabolic process; F:transferase activity; F:ligase activity	EC:6.4.1.3; EC:2; EC:6.4.1.2	propionyl-CoA carboxylase; Transferases; acetyl-CoA carboxylase
group_2494	26	0	0	PTS glucose transporter subunit IIA	P:GO:0055085; F:GO:0005215; F:GO:0016740	P:transmembrane transport; F:transporter activity; F:transferase activity	EC:2.7.1	Transferring phosphorus-containing groups
rssB_2	27	1	2	two-component system response	P:GO:0023052	P:signaling		

				regulator YesN[a]		
yveA_2	27	1	3	aspartate/proton symporter AspP	P:GO:0055085; F:GO:0005215	P:transmembrane transport; F:transporter activity

[1]"SeqName" is the name assigned by the Roary analysis. [2]"The number in broad-sense natto group" includes the count for the Bekang strain. [3]"Description" refers to the annotation in the sequence similarity search. [a]*rssB* and *yesN* are synonyms for the same gene.

622 **Table 3.** A selection of nearly "natto-related group"-specific genes.

SeqName[1]	The number broad-sense natto group [2]	Presence in Bekang strain (1/0)	The number in Group B	Description[3]	GO IDs	GO Names	Enzyme Codes	Enzyme Names
sigV_2	0	0	14	sigma-70 family RNA polymerase sigma factor	P:GO:0006355; F:GO:0003677; F:GO:0140110	P:regulation of DNA-templated transcription; F:DNA binding; F:transcription regulator activity		
yedK	0	0	12	SOS response-associated peptidase	P:GO:0006281; F:GO:0003677	P:DNA repair; F:DNA binding		
group_2711	0	0	12	helix-turn-helix transcriptional regulator	F:GO:0003677	F:DNA binding		
group_6178	4	0	13	IS21 family transposase	P:GO:0006310; F:GO:0003677; F:GO:0140097	P:DNA recombination; F:DNA binding; F:catalytic activity, acting on DNA		
rapI_4	0	0	13	tetratricopeptide repeat protein	F:GO:0005515	F:protein binding		
rsoA	0	0	12	sigma-O factor regulator RsoA	F:GO:0005515	F:protein binding		
group_393	3	0	15	M20/M25/M40 family metallo-hydrolase	F:GO:0016787	F:hydrolase activity	EC:3	Hydrolases
group_1244	5	0	12	ATP-dependent helicase	F:GO:0016787	F:hydrolase activity	EC:3	Hydrolases
group_2724	0	0	12	N-acetylmuramoyl-L-alanine amidase	P:GO:1901135; F:GO:0016787	P:carbohydrate derivative metabolic process; F:hydrolase activity	EC:3.5.1.28	N-acetylmuramoyl-L-alanine amidase
group_2746	0	0	12	Fe(3+)-citrate ABC transporter ATP-binding protein YfmF	F:GO:0016787; F:GO:0140657	F:hydrolase activity; F:ATP-dependent activity	EC:3.6.1.15	nucleoside-triphosphate phosphatase
spoVAD_1	0	0	12	stage V sporulation protein AD	F:GO:0016740	F:transferase activity	EC:2.3	Acyltransferases
uhpB	1	1	12	sensor histidine kinase	P:GO:0023052; F:GO:0016740;	P:signaling; F:transferase activity;	EC:2.7.3; EC:2.7.13.3	Transferring phosphorus-containing

					F:GO:0140096; F:GO:0140299	F:catalytic activity, acting on a protein; F:molecular sensor activity		groups; histidine kinase
ydaF_2	0	0	13	GNAT family protein	F:GO:0016740	F:transferase activity	EC:2.3.1	Acyltransferases
yoaC	0	0	13	FGGY-family carbohydrate kinase	P:GO:0005975; F:GO:0016740	P:carbohydrate metabolic process; F:transferase activity	EC:2.7	Transferring phosphorus-containing groups
group_96	2	1	14	peptidoglycan O-acetyltransferase OatA	P:GO:0005975; P:GO:0006629; P:GO:1901135; F:GO:0016740; C:GO:0005886	P:carbohydrate metabolic process; P:lipid metabolic process; P:carbohydrate derivative metabolic process; F:transferase activity; C:plasma membrane	EC:2.3.1	Acyltransferases
group_428	2	1	12	type III polyketide synthase BpsA	F:GO:0016740	F:transferase activity	EC:2.3	Acyltransferases
group_2741	0	0	12	8-amino-7-oxononanoate synthase	P:GO:0006766; P:GO:0006790; F:GO:0016740	P:vitamin metabolic process; P:sulfur compound metabolic process; F:transferase activity	EC:2.3.1.47	8-amino-7-oxononanoate synthase
group_3003	0	0	12	GNAT family N-acetyltransferase	F:GO:0016740	F:transferase activity	EC:2.3.1	Acyltransferases
group_2736	0	0	13	phospholipase D-like domain-containing protein	F:GO:0003824	F:catalytic activity		
group_3006	0	0	15	T7SS effector LXG polymorphic toxin	F:GO:0003824	F:catalytic activity		
group_2720	0	0	12	4-hydroxyphenylacetate 3-monooxygenase, .oxygenase component	F:GO:0016491	F:oxidoreductase activity	EC:1.3; EC:1.14.14	Acting on the CH-CH group of donors; Acting on paired donors, with incorporation or reduction of molecular oxygen. The oxygen incorporated

								need not be derived from O2
alkH	0	0	12	aldehyde dehydrogenase family protein	F:GO:0016491	F:oxidoreductase activity	EC:1.2.1	Acting on the aldehyde or oxo group of donors
yfmJ	0	0	12	NADP-dependent oxidoreductase	F:GO:0016491	F:oxidoreductase activity	EC:1.3.1	Acting on the CH-CH group of donors
pelB_2	0	0	12	polysaccharide lyase family 1 protein	P:GO:0005975; F:GO:0016829; C:GO:0005576	P:carbohydrate metabolic process; F:lyase activity; C:extracellular region	EC:4.2.2.2	pectate lyase
yxxD	0	0	13	type II toxin-antitoxin system antitoxin YxxD	C:GO:0005737	C:cytoplasm		
group_2719	0	0	12	YoaK family protein	C:GO:0005886	C:plasma membrane		
group_2712	0	0	12	DUF2975 domain-containing protein	C:GO:0005886	C:plasma membrane		
group_1989	0	0	12	DUF421 domain-containing protein	C:GO:0005886	C:plasma membrane		
group_3077	0	0	12	RDD family protein	C:GO:0005886	C:plasma membrane		
group_3076	0	0	12	DUF5391 family protein	C:GO:0005886	C:plasma membrane		
group_2664	1	1	15	DUF2892 domain-containing protein	C:GO:0005886	C:plasma membrane		
group_2665	1	1	14	NP_388648.1 conserved membrane protein	C:GO:0005886	C:plasma membrane		
group_1986	0	0	12	Uncharacterised protein	C:GO:0016020	C:membrane		
yoaH	0	0	12	methyl-accepting chemotaxis protein	C:GO:0016020	C:membrane		
group_2716	0	0	12	DUF4944 domain-containing protein	C:GO:0016020	C:membrane		
group_3078	0	0	12	DUF418 domain-containing protein	C:GO:0016020	C:membrane		
group_2733	0	0	12	MULTISPECIES: stage V sporulation protein AE	C:GO:0016020	C:membrane		
group_2731	0	0	12	stage V sporulation protein AC	C:GO:0016020	C:membrane		
group_3007	0	0	15	KFK80766.1 putative membrane protein	C:GO:0016020	C:membrane		

group_631	1	1	15	YgcG family protein	C:GO:0016020	C:membrane
group_2672	1	1	13	YpfB family protein	C:GO:0016020	C:membrane
group_385	4	1	14	MFS transporter	C:GO:0016020	C:membrane
yfiZ_1	0	0	12	Fe(3+) dicitrate ABC transporter permease FecD	F:GO:0005215	F:transporter activity
fecD	0	0	12	Fe(3+)-citrate ABC transporter permease YfmE	F:GO:0005215	F:transporter activity
group_303	2	1	14	iron ABC transporter permease	F:GO:0005215	F:transporter activity
gerXA_1	0	0	12	Spore germination protein	P:GO:0009847; C:GO:0016020	P:spore germination; C:membrane
group_2742	0	0	15	sugar ABC transporter permease	P:GO:0055085	P:transmembrane transport
group_341	0	0	14	aspartate/proton symporter AspP	P:GO:0055085; F:GO:0005215	P:transmembrane transport; F:transporter activity
group_1149	1	1	13	GABA permease	P:GO:0055085; F:GO:0005215	P:transmembrane transport; F:transporter activity
group_5097	4	0	13	IS21-like element helper ATPase IstB	F:GO:0005524	F:ATP binding
oxdD	0	0	12	Oxalate decarboxylase	P:GO:0033609	P:oxalate metabolic process

[1]"SeqName" is the name assigned by the Roary analysis. [2]"The number in broad-sense natto group" includes the count for the Bekang strain. [3]"Description" refers to the annotation in the sequence similarity search.

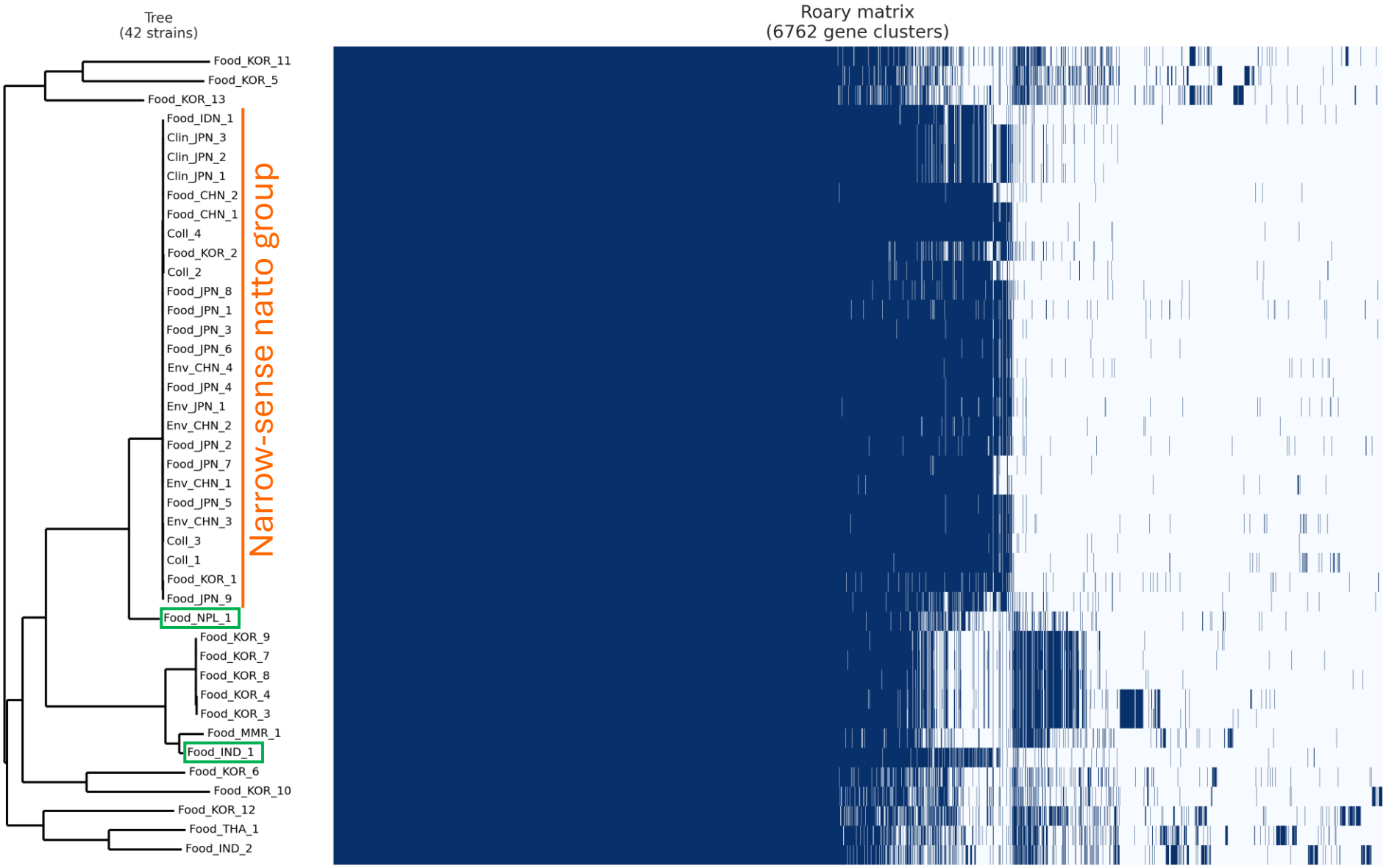
Tree
(42 strains)
Roary matrix
(6762 gene clusters)
Food_KOR_11
Food_KOR_5
Food_KOR_13
Food_IDN_1
Clin_JPN_3
Clin_JPN_2
Clin_JPN_1
Food_CHN_2
Food_CHN_1
Coll_4
Food_KOR_2
Coll_2
Food_JPN_8
Food_JPN_1
Food_JPN_3
Food_JPN_6
Env_CHN_4
Food_JPN_4
Env_JPN_1
Env_CHN_2
Food_JPN_2
Food_JPN_7
Env_CHN_1
Food_JPN_5
Env_CHN_3
Coll_3
Coll_1
Food_KOR_1
Food_JPN_9
Narrow-sense natto group
Food_NPL_1
Food_KOR_9
Food_KOR_7
Food_KOR_8
Food_KOR_4
Food_KOR_3
Food_MMR_1
Food_IND_1
Food_KOR_6
Food_KOR_10
Food_KOR_12
Food_THA_1
Food_IND_2

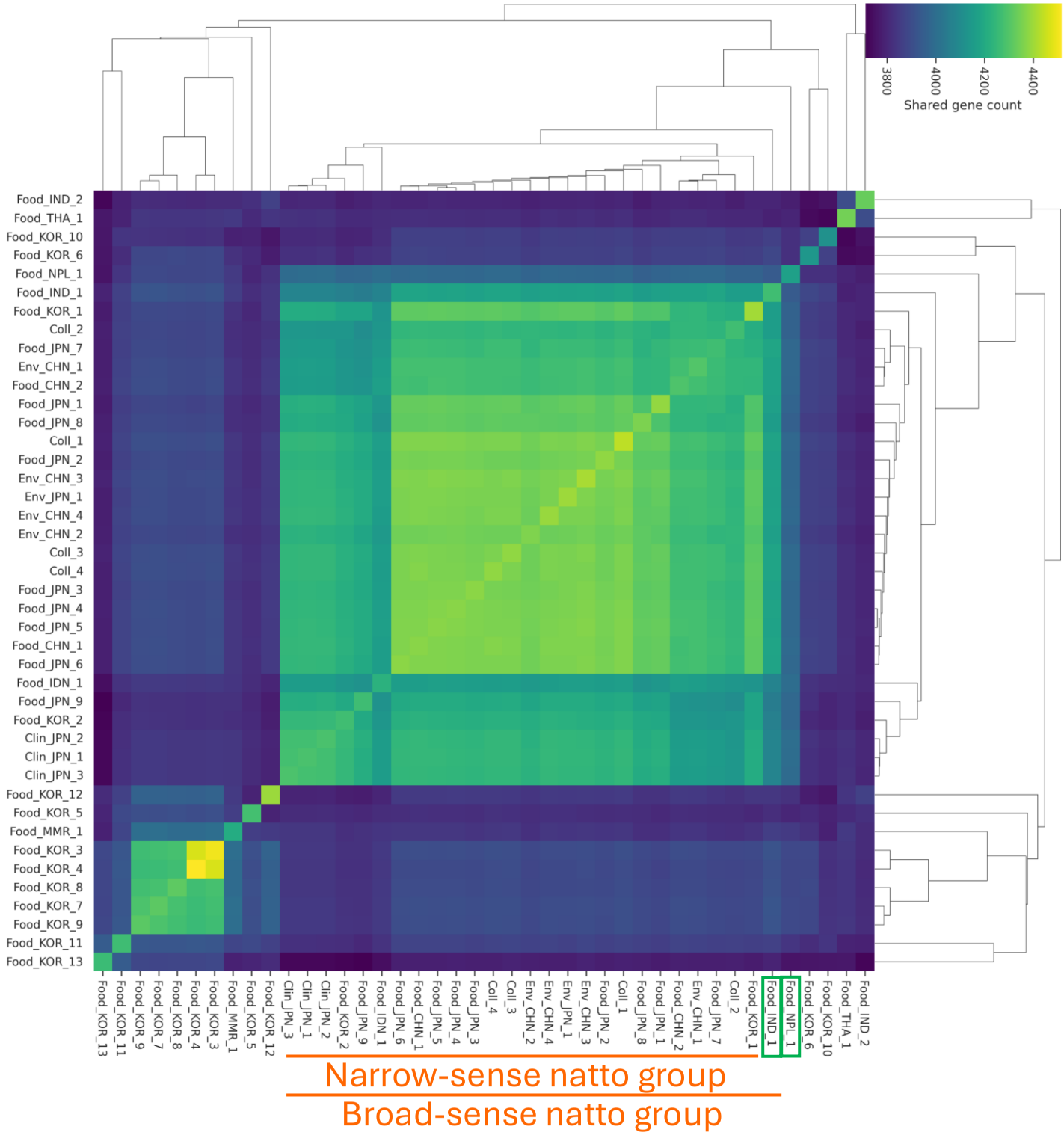
3800
4000
4200
4400
Shared gene count
Food_IND_2
Food_THA_1
Food_KOR_10
Food_KOR_6
Food_NPL_1
Food_IND_1
Food_KOR_1
Coll_2
Food_JPN_7
Env_CHN_1
Food_CHN_2
Food_JPN_1
Food_JPN_8
Coll_1
Food_JPN_2
Env_CHN_3
Env_JPN_1
Env_CHN_4
Env_CHN_2
Coll_3
Coll_4
Food_JPN_3
Food_JPN_4
Food_JPN_5
Food_CHN_1
Food_JPN_6
Food_IDN_1
Food_JPN_9
Food_KOR_2
Clin_JPN_2
Clin_JPN_1
Clin_JPN_3
Food_KOR_12
Food_KOR_5
Food_MMR_1
Food_KOR_3
Food_KOR_4
Food_KOR_8
Food_KOR_7
Food_KOR_9
Food_KOR_11
Food_KOR_13
Narrow-sense natto group
Broad-sense natto group

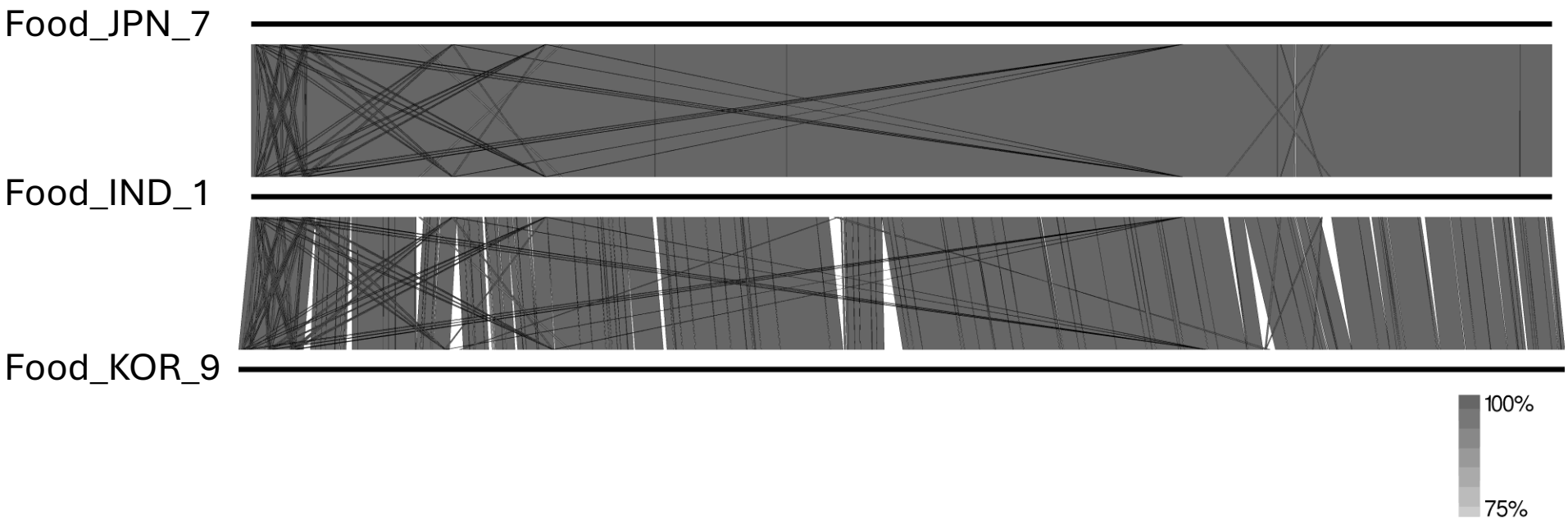
Food_JPN_7
Food_IND_1
Food_KOR_9
100%
75%

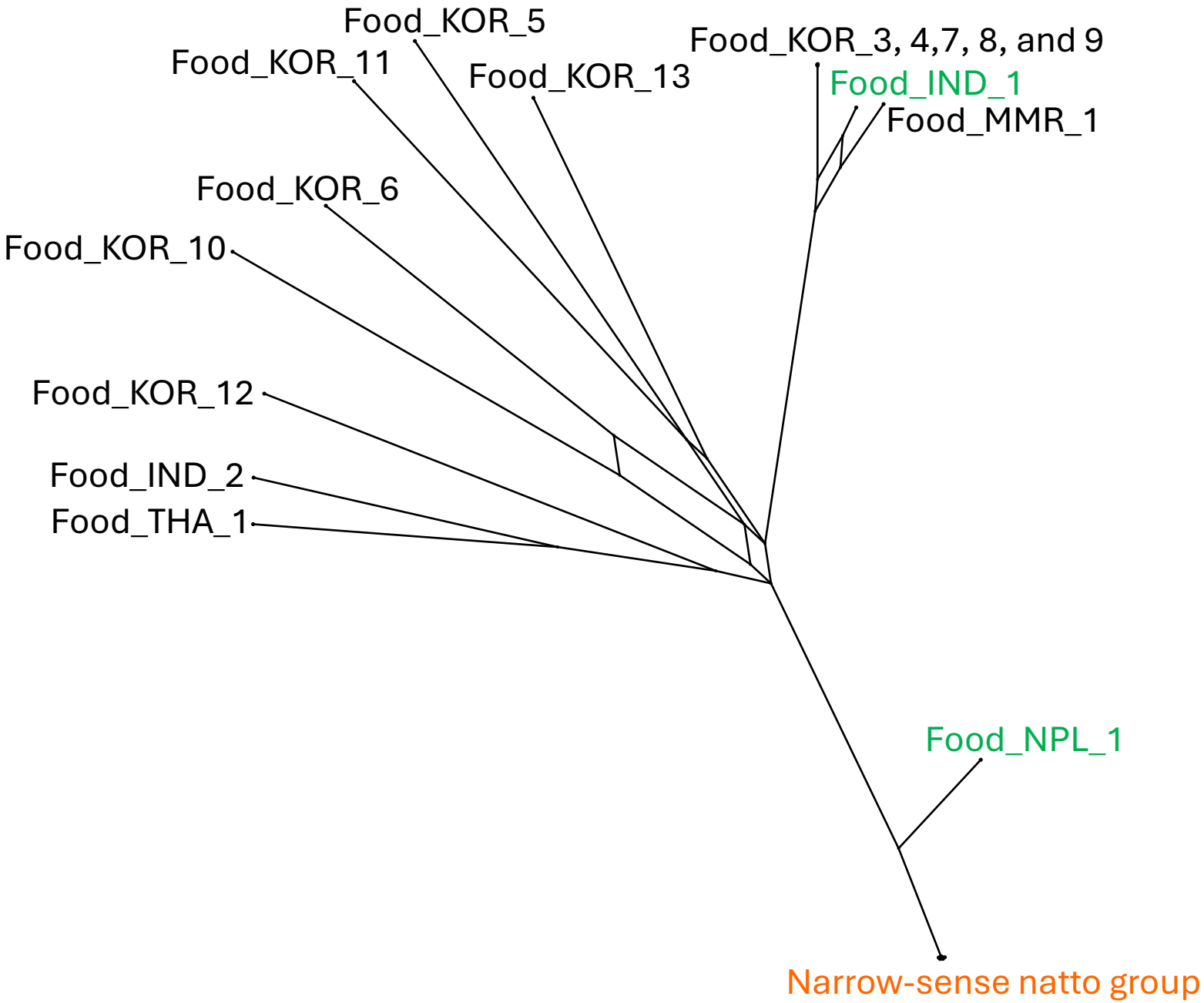
Food_KOR_5
Food_KOR_11
Food_KOR_13
Food_KOR_3, 4,7, 8, and 9
Food_IND_1
Food_MMR_1
Food_KOR_6
Food_KOR_10
Food_KOR_12
Food_IND_2
Food_THA_1
Food_NPL_1
Narrow-sense natto group

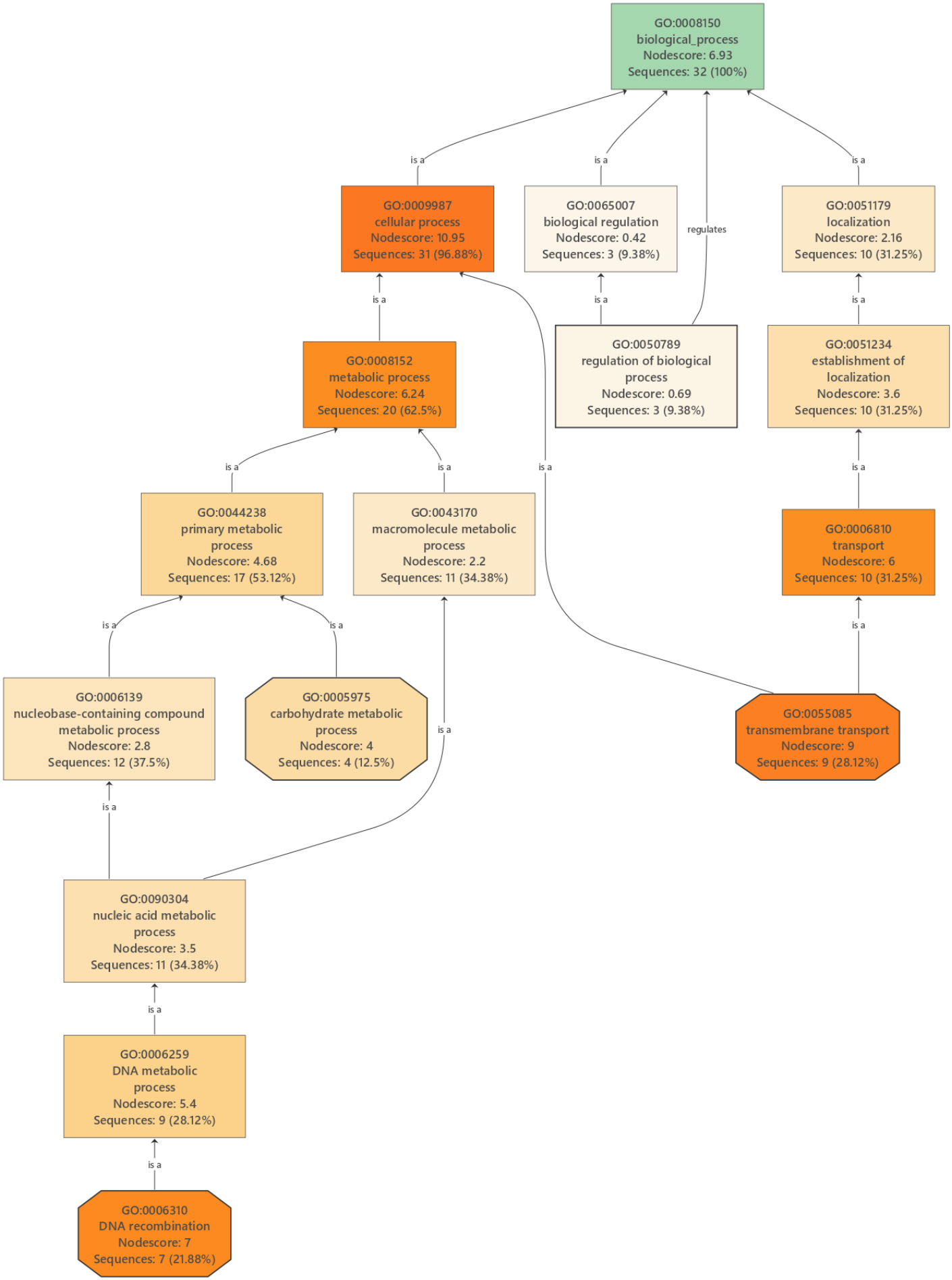
GO:0008150
biological_process
Nodescore: 6.93
Sequences: 32 (100%)
is a
is a
is a
GO:0009987
cellular process
Nodescore: 10.95
Sequences: 31 (96.88%)
GO:0065007
biological regulation
Nodescore: 0.42
Sequences: 3 (9.38%)
regulates
GO:0051179
localization
Nodescore: 2.16
Sequences: 10 (31.25%)
is a
is a
is a
GO:0008152
metabolic process
Nodescore: 6.24
Sequences: 20 (62.5%)
GO:0050789
regulation of biological process
Nodescore: 0.69
Sequences: 3 (9.38%)
GO:0051234
establishment of localization
Nodescore: 3.6
Sequences: 10 (31.25%)
is a
is a
is a
is a
GO:0044238
primary metabolic process
Nodescore: 4.68
Sequences: 17 (53.12%)
GO:0043170
macromolecule metabolic process
Nodescore: 2.2
Sequences: 11 (34.38%)
GO:0006810
transport
Nodescore: 6
Sequences: 10 (31.25%)
is a
is a
is a
is a
GO:0006139
nucleobase-containing compound metabolic process
Nodescore: 2.8
Sequences: 12 (37.5%)
GO:0005975
carbohydrate metabolic process
Nodescore: 4
Sequences: 4 (12.5%)
GO:0055085
transmembrane transport
Nodescore: 9
Sequences: 9 (28.12%)
is a
is a
GO:0090304
nucleic acid metabolic process
Nodescore: 3.5
Sequences: 11 (34.38%)
is a
GO:0006259
DNA metabolic process
Nodescore: 5.4
Sequences: 9 (28.12%)
is a
GO:0006310
DNA recombination
Nodescore: 7
Sequences: 7 (21.88%)

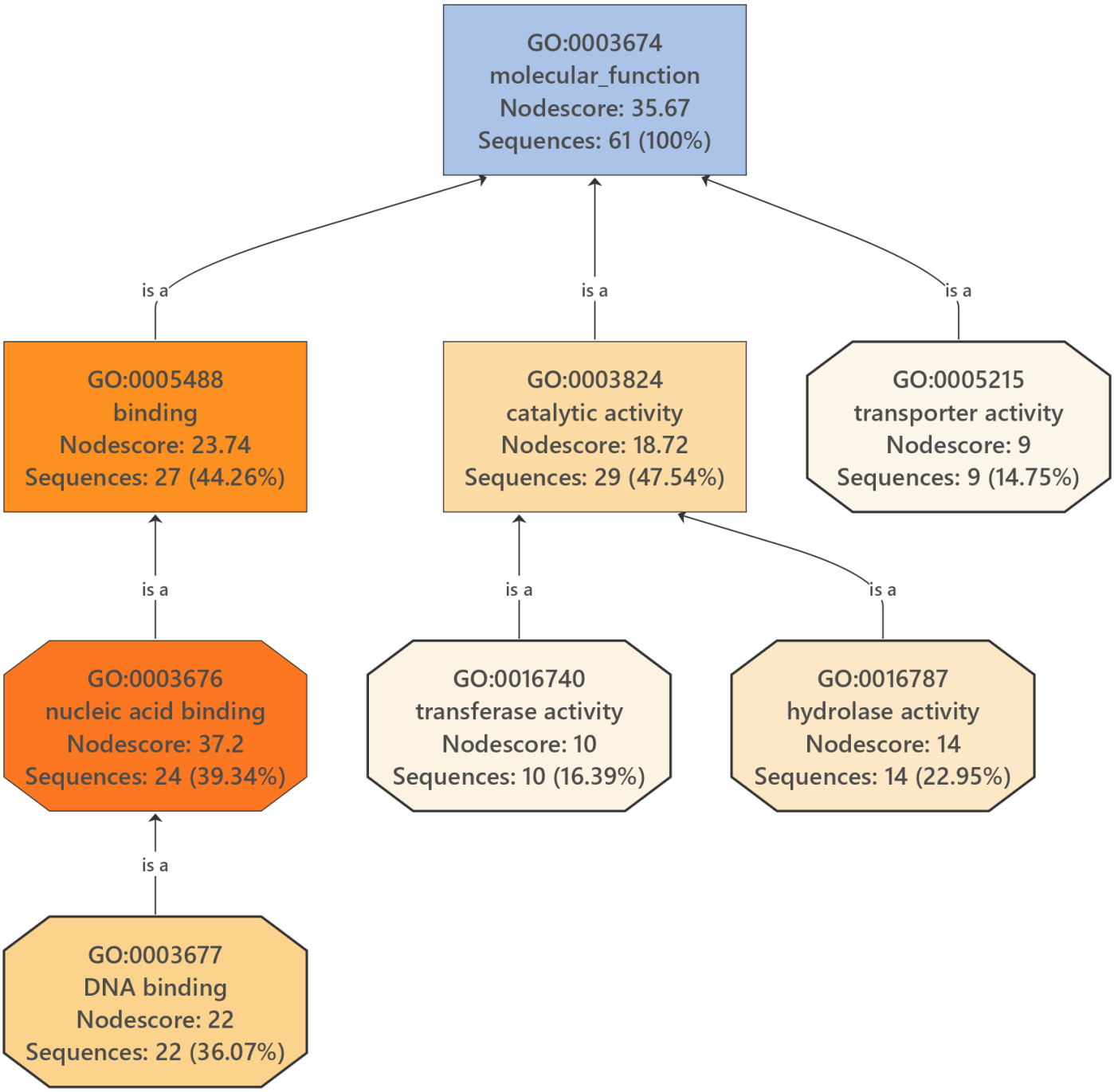
GO:0003674
molecular_function
Nodescore: 35.67
Sequences: 61 (100%)
is a
is a
is a
GO:0005488
binding
Nodescore: 23.74
Sequences: 27 (44.26%)
GO:0003824
catalytic activity
Nodescore: 18.72
Sequences: 29 (47.54%)
GO:0005215
transporter activity
Nodescore: 9
Sequences: 9 (14.75%)
is a
is a
is a
GO:0003676
nucleic acid binding
Nodescore: 37.2
Sequences: 24 (39.34%)
GO:0016740
transferase activity
Nodescore: 10
Sequences: 10 (16.39%)
GO:0016787
hydrolase activity
Nodescore: 14
Sequences: 14 (22.95%)
is a
GO:0003677
DNA binding
Nodescore: 22
Sequences: 22 (36.07%)